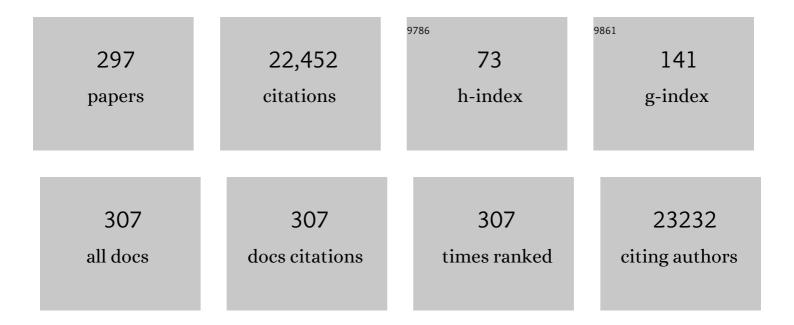
List of Publications by Year in descending order

Source: https://exaly.com/author-pdf/3443442/publications.pdf

Version: 2024-02-01



MIRKO PRATO

#	Article	IF	CITATIONS
1	Tuning the Optical Properties of Cesium Lead Halide Perovskite Nanocrystals by Anion Exchange Reactions. Journal of the American Chemical Society, 2015, 137, 10276-10281.	13.7	1,765
2	The Einstein Telescope: a third-generation gravitational wave observatory. Classical and Quantum Gravity, 2010, 27, 194002.	4.0	1,211
3	Predictions for the rates of compact binary coalescences observable by ground-based gravitational-wave detectors. Classical and Quantum Gravity, 2010, 27, 173001.	4.0	956
4	Solution Synthesis Approach to Colloidal Cesium Lead Halide Perovskite Nanoplatelets with Monolayer-Level Thickness Control. Journal of the American Chemical Society, 2016, 138, 1010-1016.	13.7	747
5	Sensitivity studies for third-generation gravitational wave observatories. Classical and Quantum Gravity, 2011, 28, 094013.	4.0	644
6	Strongly emissive perovskite nanocrystal inks for high-voltage solar cells. Nature Energy, 2017, 2, .	39.5	544
7	Benzoyl Halides as Alternative Precursors for the Colloidal Synthesis of Lead-Based Halide Perovskite Nanocrystals. Journal of the American Chemical Society, 2018, 140, 2656-2664.	13.7	490
8	Nearly Monodisperse Insulator Cs ₄ PbX ₆ (X = Cl, Br, I) Nanocrystals, Their Mixed Halide Compositions, and Their Transformation into CsPbX ₃ Nanocrystals. Nano Letters, 2017, 17, 1924-1930.	9.1	488
9	Colloidal Synthesis of Quantum Confined Single Crystal CsPbBr ₃ Nanosheets with Lateral Size Control up to the Micrometer Range. Journal of the American Chemical Society, 2016, 138, 7240-7243.	13.7	446
10	Colloidal Synthesis of Double Perovskite Cs ₂ AgInCl ₆ and Mn-Doped Cs ₂ AgInCl ₆ Nanocrystals. Journal of the American Chemical Society, 2018, 140, 12989-12995.	13.7	397
11	Copper Sulfide Nanocrystals with Tunable Composition by Reduction of Covellite Nanocrystals with Cu ⁺ Ions. Journal of the American Chemical Society, 2013, 135, 17630-17637.	13.7	377
12	Scientific objectives of Einstein Telescope. Classical and Quantum Gravity, 2012, 29, 124013.	4.0	355
13	X-ray Lithography on Perovskite Nanocrystals Films: From Patterning with Anion-Exchange Reactions to Enhanced Stability in Air and Water. ACS Nano, 2016, 10, 1224-1230.	14.6	320
14	Strongly Fluorescent Quaternary Cu–In–Zn–S Nanocrystals Prepared from Cu _{1-<i>x</i>} InS ₂ Nanocrystals by Partial Cation Exchange. Chemistry of Materials, 2012, 24, 2400-2406.	6.7	291
15	The third generation of gravitational wave observatories and their science reach. Classical and Quantum Gravity, 2010, 27, 084007.	4.0	287
16	Virgo: a laser interferometer to detect gravitational waves. Journal of Instrumentation, 2012, 7, P03012-P03012.	1.2	257
17	<i>In Situ</i> Transmission Electron Microscopy Study of Electron Beam-Induced Transformations in Colloidal Cesium Lead Halide Perovskite Nanocrystals. ACS Nano, 2017, 11, 2124-2132.	14.6	246
18	The Impact of the Crystallization Processes on the Structural and Optical Properties of Hybrid Perovskite Films for Photovoltaics. Journal of Physical Chemistry Letters, 2014, 5, 3836-3842.	4.6	238

#	Article	IF	CITATIONS
19	Colloidal Synthesis of Strongly Fluorescent CsPbBr ₃ Nanowires with Width Tunable down to the Quantum Confinement Regime. Chemistry of Materials, 2016, 28, 6450-6454.	6.7	219
20	Few‣ayer MoS ₂ Flakes as Active Buffer Layer for Stable Perovskite Solar Cells. Advanced Energy Materials, 2016, 6, 1600920.	19.5	207
21	MoS ₂ Quantum Dot/Graphene Hybrids for Advanced Interface Engineering of a CH ₃ NH ₃ Pbl ₃ Perovskite Solar Cell with an Efficiency of over 20%. ACS Nano, 2018, 12, 10736-10754.	14.6	201
22	Emissive Bi-Doped Double Perovskite Cs ₂ Ag _{1–<i>x</i>} Na _{<i>x</i>} InCl ₆ Nanocrystals. ACS Energy Letters, 2019, 4, 1976-1982.	17.4	198
23	Search for gravitational waves from low mass compact binary coalescence in LIGO's sixth science run and Virgo's science runs 2 and 3. Physical Review D, 2012, 85, .	4.7	185
24	Light-assisted delithiation of lithium iron phosphate nanocrystals towards photo-rechargeable lithium ion batteries. Nature Communications, 2017, 8, 14643.	12.8	179
25	Postsynthesis Transformation of Insulating Cs ₄ PbBr ₆ Nanocrystals into Bright Perovskite CsPbBr ₃ through Physical and Chemical Extraction of CsBr. ACS Energy Letters, 2017, 2, 2445-2448.	17.4	177
26	Scalable Production of Graphene Inks via Wetâ€Jet Milling Exfoliation for Screenâ€Printed Micro‣upercapacitors. Advanced Functional Materials, 2019, 29, 1807659.	14.9	174
27	From Binary Cu ₂ S to Ternary Cu–In–S and Quaternary Cu–In–Zn–S Nanocrystals with Tunable Composition <i>via</i> Partial Cation Exchange. ACS Nano, 2015, 9, 521-531.	14.6	173
28	Simultaneous Cationic and Anionic Ligand Exchange For Colloidally Stable CsPbBr ₃ Nanocrystals. ACS Energy Letters, 2019, 4, 819-824.	17.4	173
29	Status of the Virgo project. Classical and Quantum Gravity, 2011, 28, 114002.	4.0	171
30	lon Migration and the Role of Preconditioning Cycles in the Stabilization of the <i>J</i> – <i>V</i> Characteristics of Inverted Hybrid Perovskite Solar Cells. Advanced Energy Materials, 2016, 6, 1501453.	19.5	167
31	SEARCHES FOR GRAVITATIONAL WAVES FROM KNOWN PULSARS WITH SCIENCE RUN 5 LIGO DATA. Astrophysical Journal, 2010, 713, 671-685.	4.5	155
32	Polymer-Free Films of Inorganic Halide Perovskite Nanocrystals as UV-to-White Color-Conversion Layers in LEDs. Chemistry of Materials, 2016, 28, 2902-2906.	6.7	152
33	Engineered MoSe ₂ â€Based Heterostructures for Efficient Electrochemical Hydrogen Evolution Reaction. Advanced Energy Materials, 2018, 8, 1703212.	19.5	152
34	Generalized One-Pot Synthesis of Copper Sulfide, Selenide-Sulfide, and Telluride-Sulfide Nanoparticles. Chemistry of Materials, 2014, 26, 1442-1449.	6.7	150
35	Changing the Dimensionality of Cesium Lead Bromide Nanocrystals by Reversible Postsynthesis Transformations with Amines. Chemistry of Materials, 2017, 29, 4167-4171.	6.7	142
36	High-yield production of 2D crystals by wet-jet milling. Materials Horizons, 2018, 5, 890-904.	12.2	139

#	Article	IF	CITATIONS
37	Synthesis of Uniform Disk-Shaped Copper Telluride Nanocrystals and Cation Exchange to Cadmium Telluride Quantum Disks with Stable Red Emission. Journal of the American Chemical Society, 2013, 135, 12270-12278.	13.7	138
38	Cu _{3-<i>x</i>} P Nanocrystals as a Material Platform for Near-Infrared Plasmonics and Cation Exchange Reactions. Chemistry of Materials, 2015, 27, 1120-1128.	6.7	137
39	Chloride-Induced Thickness Control in CdSe Nanoplatelets. Nano Letters, 2018, 18, 6248-6254.	9.1	135
40	Parameter estimation for compact binary coalescence signals with the first generation gravitational-wave detector network. Physical Review D, 2013, 88, .	4.7	132
41	Shape-Pure, Nearly Monodispersed CsPbBr ₃ Nanocubes Prepared Using Secondary Aliphatic Amines. Nano Letters, 2018, 18, 7822-7831.	9.1	132
42	Two-Dimensional Material Interface Engineering for Efficient Perovskite Large-Area Modules. ACS Energy Letters, 2019, 4, 1862-1871.	17.4	125
43	Alloyed Copper Chalcogenide Nanoplatelets <i>via</i> Partial Cation Exchange Reactions. ACS Nano, 2014, 8, 8407-8418.	14.6	123
44	Carbon Nanotube-Supported MoSe ₂ Holey Flake:Mo ₂ C Ball Hybrids for Bifunctional pH-Universal Water Splitting. ACS Nano, 2019, 13, 3162-3176.	14.6	120
45	Tuning the Lattice Parameter of In _{<i>x</i>} Zn _{<i>y</i>} P for Highly Luminescent Lattice-Matched Core/Shell Quantum Dots. ACS Nano, 2016, 10, 4754-4762.	14.6	117
46	Search for gravitational waves from compact binary coalescence in LIGO and Virgo data from S5 and VSR1. Physical Review D, 2010, 82, .	4.7	111
47	All-sky search for gravitational-wave bursts in the first joint LIGO-GEO-Virgo run. Physical Review D, 2010, 81, .	4.7	107
48	All-sky search for gravitational-wave bursts in the second joint LIGO-Virgo run. Physical Review D, 2012, 85, .	4.7	107
49	SEARCH FOR GRAVITATIONAL WAVES ASSOCIATED WITH GAMMA-RAY BURSTS DURING LIGO SCIENCE RUN 6 AND VIRGO SCIENCE RUNS 2 AND 3. Astrophysical Journal, 2012, 760, 12.	4.5	104
50	The effect of silver oxidation on the photocatalytic activity of Ag/ZnO hybrid plasmonic/metal-oxide nanostructures under visible light and in the dark. Scientific Reports, 2019, 9, 11839.	3.3	104
51	Role of Nonradiative Defects and Environmental Oxygen on Exciton Recombination Processes in CsPbBr ₃ Perovskite Nanocrystals. Nano Letters, 2017, 17, 3844-3853.	9.1	101
52	From CsPbBr ₃ Nano-Inks to Sintered CsPbBr ₃ –CsPb ₂ Br ₅ Films via Thermal Annealing: Implications on Optoelectronic Properties. Journal of Physical Chemistry C, 2017, 121, 11956-11961.	3.1	96
53	Directional Limits on Persistent Gravitational Waves Using LIGO S5 Science Data. Physical Review Letters, 2011, 107, 271102.	7.8	94
54	Hollow and Porous Nickel Cobalt Perselenide Nanostructured Microparticles for Enhanced Electrocatalytic Oxygen Evolution. Chemistry of Materials, 2017, 29, 7032-7041.	6.7	93

#	Article	IF	CITATIONS
55	Solution-Processed Hybrid Graphene Flake/2H-MoS ₂ Quantum Dot Heterostructures for Efficient Electrochemical Hydrogen Evolution. Chemistry of Materials, 2017, 29, 5782-5786.	6.7	93
56	Search for gravitational waves from binary black hole inspiral, merger, and ringdown in LIGO-Virgo data from 2009–2010. Physical Review D, 2013, 87, .	4.7	92
57	Einstein@Home all-sky search for periodic gravitational waves in LIGO S5 data. Physical Review D, 2013, 87, .	4.7	91
58	SEARCH FOR GRAVITATIONAL-WAVE INSPIRAL SIGNALS ASSOCIATED WITH SHORT GAMMA-RAY BURSTS DURING LIGO'S FIFTH AND VIRGO'S FIRST SCIENCE RUN. Astrophysical Journal, 2010, 715, 1453-1461.	4.5	90
59	Size-Tuning of WSe ₂ Flakes for High Efficiency Inverted Organic Solar Cells. ACS Nano, 2017, 11, 3517-3531.	14.6	90
60	Liquidâ€Phase Exfoliated Indium–Selenide Flakes and Their Application in Hydrogen Evolution Reaction. Small, 2018, 14, e1800749.	10.0	90
61	BEATING THE SPIN-DOWN LIMIT ON GRAVITATIONAL WAVE EMISSION FROM THE VELA PULSAR. Astrophysical Journal, 2011, 737, 93.	4.5	89
62	Nanoscale Transformations in Covellite (CuS) Nanocrystals in the Presence of Divalent Metal Cations in a Mild Reducing Environment. Chemistry of Materials, 2015, 27, 7531-7537.	6.7	89
63	WS ₂ –Graphite Dual-Ion Batteries. Nano Letters, 2018, 18, 7155-7164.	9.1	88
64	Squeezing Terahertz Light into Nanovolumes: Nanoantenna Enhanced Terahertz Spectroscopy (NETS) of Semiconductor Quantum Dots. Nano Letters, 2015, 15, 386-391.	9.1	86
65	Boosting Perovskite Solar Cells Performance and Stability through Doping a Polyâ€3(hexylthiophene) Hole Transporting Material with Organic Functionalized Carbon Nanostructures. Advanced Functional Materials, 2016, 26, 7443-7453.	14.9	86
66	Search for gravitational waves from binary black hole inspiral, merger, and ringdown. Physical Review D, 2011, 83, .	4.7	85
67	Calibration and sensitivity of the Virgo detector during its second science run. Classical and Quantum Gravity, 2011, 28, 025005.	4.0	85
68	Implementation and testing of the first prompt search forÂgravitational wave transients with electromagnetic counterparts. Astronomy and Astrophysics, 2012, 539, A124.	5.1	84
69	Liquid repellent nanocomposites obtained from one-step water-based spray. Journal of Materials Chemistry A, 2015, 3, 12880-12889.	10.3	81
70	Self-Assembly of 1,4-Benzenedimethanethiol Self-Assembled Monolayers on Gold. Langmuir, 2010, 26, 7242-7247.	3.5	80
71	Binder-free graphene as an advanced anode for lithium batteries. Journal of Materials Chemistry A, 2016, 4, 6886-6895.	10.3	79
72	First low-latency LIGO+Virgo search for binary inspirals and their electromagnetic counterparts. Astronomy and Astrophysics, 2012, 541, A155.	5.1	75

#	Article	IF	CITATIONS
73	The characterization of Virgo data and its impact on gravitational-wave searches. Classical and Quantum Gravity, 2012, 29, 155002.	4.0	73
74	Nonlinear Carrier Interactions in Lead Halide Perovskites and the Role of Defects. Journal of the American Chemical Society, 2016, 138, 13604-13611.	13.7	73
75	Optical Characterization of Thiolate Self-Assembled Monolayers on Au(111). Journal of Physical Chemistry C, 2008, 112, 3899-3906.	3.1	70
76	Colloidal Cu2â˜x(SySe1☒y) alloy nanocrystals with controllable crystal phase: synthesis, plasmonic properties, cation exchange and electrochemical lithiation. Journal of Materials Chemistry, 2012, 22, 13023.	6.7	70
77	Stimuli-responsive lipid-based magnetic nanovectors increase apoptosis in glioblastoma cells through synergic intracellular hyperthermia and chemotherapy. Nanoscale, 2019, 11, 72-88.	5.6	69
78	Homotypic targeting and drug delivery in glioblastoma cells through cell membrane-coated boron nitride nanotubes. Materials and Design, 2020, 192, 108742.	7.0	69
79	Reduction of moisture sensitivity of PbS quantum dot solar cells by incorporation of reduced graphene oxide. Solar Energy Materials and Solar Cells, 2018, 183, 1-7.	6.2	68
80	Dopedâ€MoSe ₂ Nanoflakes/3d Metal Oxide–Hydr(Oxy)Oxides Hybrid Catalysts for pHâ€Universal Electrochemical Hydrogen Evolution Reaction. Advanced Energy Materials, 2018, 8, 1801764.	19.5	67
81	All-sky search for periodic gravitational waves in the full S5 LIGO data. Physical Review D, 2012, 85, .	4.7	66
82	Colloidal Synthesis of Cuprite (Cu ₂ O) Octahedral Nanocrystals and Their Electrochemical Lithiation. ACS Applied Materials & Interfaces, 2013, 5, 2745-2751.	8.0	66
83	Integration of two-dimensional materials-based perovskite solar panels into a stand-alone solar farm. Nature Energy, 2022, 7, 597-607.	39.5	66
84	Culn _{<i>x</i>} Ga _{1–<i>x</i>} S ₂ Nanocrystals with Tunable Composition and Band Gap Synthesized via a Phosphine-Free and Scalable Procedure. Chemistry of Materials, 2013, 25, 3180-3187.	6.7	65
85	Direct Synthesis of Carbon-Doped TiO ₂ –Bronze Nanowires as Anode Materials for High Performance Lithium-Ion Batteries. ACS Applied Materials & Interfaces, 2015, 7, 25139-25146.	8.0	65
86	Influence of Chloride Ions on the Synthesis of Colloidal Branched CdSe/CdS Nanocrystals by Seeded Growth. ACS Nano, 2012, 6, 11088-11096.	14.6	64
87	On the self assembly of short chain alkanedithiols. Physical Chemistry Chemical Physics, 2008, 10, 6836.	2.8	62
88	Measurements of Superattenuator seismic isolation by Virgo interferometer. Astroparticle Physics, 2010, 33, 182-189.	4.3	62
89	SWIFT FOLLOW-UP OBSERVATIONS OF CANDIDATE GRAVITATIONAL-WAVE TRANSIENT EVENTS. Astrophysical Journal, Supplement Series, 2012, 203, 28.	7.7	62
90	Evolution of CsPbBr ₃ nanocrystals upon post-synthesis annealing under an inert atmosphere. Journal of Materials Chemistry C, 2016, 4, 9179-9182.	5.5	62

#	Article	IF	CITATIONS
91	Green-Emitting Powders of Zero-Dimensional Cs ₄ PbBr ₆ : Delineating the Intricacies of the Synthesis and the Origin of Photoluminescence. Chemistry of Materials, 2019, 31, 7761-7769.	6.7	62
92	New Stereocomplex PLA-Based Fibers: Effect of POSS on Polymer Functionalization and Properties. Macromolecules, 2014, 47, 4718-4727.	4.8	61
93	Scalable spray-coated graphene-based electrodes for high-power electrochemical double-layer capacitors operating over a wide range of temperature. Energy Storage Materials, 2021, 34, 1-11.	18.0	61
94	SEARCH FOR GRAVITATIONAL-WAVE BURSTS ASSOCIATED WITH GAMMA-RAY BURSTS USING DATA FROM LIGO SCIENCE RUN 5 AND VIRGO SCIENCE RUN 1. Astrophysical Journal, 2010, 715, 1438-1452.	4.5	60
95	TaS ₂ , TaSe ₂ , and Their Heterogeneous Films as Catalysts for the Hydrogen Evolution Reaction. ACS Catalysis, 2020, 10, 3313-3325.	11.2	60
96	Noise from scattered light in Virgo's second science run data. Classical and Quantum Gravity, 2010, 27, 194011.	4.0	59
97	CO Oxidation on Colloidal Au _{0.80} Pd _{0.20} –Fe _{<i>x</i>} O _{<i>y</i>} Dumbbell Nanocrystals. Nano Letters, 2013, 13, 752-757.	9.1	57
98	Nitrogen-Doped Single-Walled Carbon Nanohorns as a Cost-Effective Carbon Host toward High-Performance Lithium–Sulfur Batteries. ACS Applied Materials & Interfaces, 2018, 10, 5551-5559.	8.0	57
99	SEARCH FOR GRAVITATIONAL WAVE BURSTS FROM SIX MAGNETARS. Astrophysical Journal Letters, 2011, 734, L35.	8.3	55
100	Enhancing the Performance of CdSe/CdS Dot-in-Rod Light-Emitting Diodes via Surface Ligand Modification. ACS Applied Materials & Interfaces, 2018, 10, 5665-5672.	8.0	55
101	Cation exchange mediated elimination of the Fe-antisites in the hydrothermal synthesis of LiFePO4. Nano Energy, 2015, 16, 256-267.	16.0	54
102	Permanent excimer superstructures by supramolecular networking of metal quantum clusters. Science, 2016, 353, 571-575.	12.6	54
103	Etched Colloidal LiFePO4 Nanoplatelets toward High-Rate Capable Li-Ion Battery Electrodes. Nano Letters, 2014, 14, 6828-6835.	9.1	53
104	Accelerated Removal of Fe-Antisite Defects while Nanosizing Hydrothermal LiFePO ₄ with Ca ²⁺ . Nano Letters, 2016, 16, 2692-2697.	9.1	52
105	Electrodeposited PEDOT:Nafion Composite for Neural Recording and Stimulation. Advanced Healthcare Materials, 2019, 8, e1900765.	7.6	51
106	Tuning and Locking the Localized Surface Plasmon Resonances of CuS (Covellite) Nanocrystals by an Amorphous CuPd _{<i>x</i>} S Shell. Chemistry of Materials, 2017, 29, 1716-1723.	6.7	50
107	Reversible Concentration-Dependent Photoluminescence Quenching and Change of Emission Color in CsPbBr ₃ Nanowires and Nanoplatelets. Journal of Physical Chemistry Letters, 2017, 8, 2725-2729.	4.6	50
108	Niobium disulphide (NbS ₂)-based (heterogeneous) electrocatalysts for an efficient hydrogen evolution reaction. Journal of Materials Chemistry A, 2019, 7, 25593-25608.	10.3	50

#	Article	IF	CITATIONS
109	H2O2-assisted photocatalysis on flower-like rutile TiO2 nanostructures: Rapid dye degradation and inactivation of bacteria. Applied Surface Science, 2016, 365, 171-179.	6.1	49
110	Search for gravitational waves from intermediate mass binary black holes. Physical Review D, 2012, 85,	4.7	48
111	Nanocrystal Film Patterning by Inhibiting Cation Exchange via Electron-Beam or X-ray Lithography. Nano Letters, 2014, 14, 2116-2122.	9.1	46
112	Alloy CsCd <i>_x</i> Pb _{1–<i>x</i>} Br ₃ Perovskite Nanocrystals: The Role of Surface Passivation in Preserving Composition and Blue Emission. Chemistry of Materials, 2020, 32, 10641-10652.	6.7	45
113	Effect of the fiber orientation on the tensile and flexural behavior of continuous carbon fiber composites made via fused filament fabrication. International Journal of Advanced Manufacturing Technology, 2021, 114, 2085-2101.	3.0	45
114	Upper limits on a stochastic gravitational-wave background using LIGO and Virgo interferometers at 600–1000ÂHz. Physical Review D, 2012, 85, .	4.7	43
115	PLA/POSS Nanofibers: A Novel System for the Immobilization of Metal Nanoparticles. ACS Applied Materials & Interfaces, 2013, 5, 7688-7692.	8.0	43
116	Efficient charge transfer in solution-processed PbS quantum dot–reduced graphene oxide hybrid materials. Journal of Materials Chemistry C, 2015, 3, 7088-7095.	5.5	43
117	Scaling of capacitance of PEDOT:PSS: volume <i>vs.</i> area. Journal of Materials Chemistry C, 2020, 8, 11252-11262.	5.5	42
118	Influence of the fluorine doping on the optical properties of CdS thin films for photovoltaic applications. Thin Solid Films, 2006, 511-512, 448-452.	1.8	41
119	Two-Dimensional Gallium Sulfide Nanoflakes for UV-Selective Photoelectrochemical-type Photodetectors. Journal of Physical Chemistry C, 2021, 125, 11857-11866.	3.1	41
120	Electronic and Geometric Characterization of thel-Cysteine Paired-Row Phase on Au(110). Langmuir, 2006, 22, 11193-11198.	3.5	40
121	Highâ€Power Graphene–Carbon Nanotube Hybrid Supercapacitors. ChemNanoMat, 2017, 3, 436-446.	2.8	39
122	Biomimetic keratin gold nanoparticle-mediated <i>in vitro</i> photothermal therapy on glioblastoma multiforme. Nanomedicine, 2021, 16, 121-138.	3.3	39
123	Extending the Colloidal Transition Metal Dichalcogenide Library to ReS ₂ Nanosheets for Application in Gas Sensing and Electrocatalysis. Small, 2019, 15, e1904670.	10.0	38
124	Lanthanide-Induced Photoluminescence in Lead-Free Cs ₂ AgBiBr ₆ Bulk Perovskite: Insights from Optical and Theoretical Investigations. Journal of Physical Chemistry Letters, 2020, 11, 8893-8900.	4.6	38
125	The effect of Au domain size on the CO oxidation catalytic activity of colloidal Au–FeOx dumbbell-like heterodimers. Journal of Catalysis, 2016, 338, 115-123.	6.2	37
126	Optical Properties of Disulfide-Functionalized Diacetylene Self-Assembled Monolayers on Gold: a Spectroscopic Ellipsometry Study. Journal of Physical Chemistry C, 2009, 113, 20683-20688.	3.1	36

#	Article	IF	CITATIONS
127	How much does size really matter? Exploring the limits of graphene as Li ion battery anode material. Solid State Communications, 2017, 251, 88-93.	1.9	36
128	Nanocatalyst/Nanoplasmonâ€Enabled Detection of Organic Mercury: A Oneâ€Minute Visual Test. Angewandte Chemie - International Edition, 2019, 58, 10285-10289.	13.8	35
129	Graphene-Based Electrodes in a Vanadium Redox Flow Battery Produced by Rapid Low-Pressure Combined Gas Plasma Treatments. Chemistry of Materials, 2021, 33, 4106-4121.	6.7	35
130	Azurin Self-Assembled Monolayers Characterized by Coupling Electrical Impedance Spectroscopy and Spectroscopic Ellipsometry. Journal of Physical Chemistry B, 2004, 108, 20263-20272.	2.6	34
131	A High Voltage Olivine Cathode for Application in Lithium″on Batteries. ChemSusChem, 2016, 9, 223-230.	6.8	34
132	Writing on Nanocrystals: Patterning Colloidal Inorganic Nanocrystal Films through Irradiation-Induced Chemical Transformations of Surface Ligands. Journal of the American Chemical Society, 2017, 139, 13250-13259.	13.7	34
133	A Short-Chain Multibranched Perfluoroalkyl Thiol for More Sustainable Hydrophobic Coatings. ACS Sustainable Chemistry and Engineering, 2018, 6, 9734-9743.	6.7	34
134	Mechanochemical Synthesis of Sn(II) and Sn(IV) lodide Perovskites and Study of Their Structural, Chemical, Thermal, Optical, and Electrical Properties. Energy Technology, 2020, 8, 1900788.	3.8	34
135	Nanocrystals of Lead Chalcohalides: A Series of Kinetically Trapped Metastable Nanostructures. Journal of the American Chemical Society, 2020, 142, 10198-10211.	13.7	34
136	Optical properties of cluster-assembled nanoporous gold films. Physical Review B, 2009, 80, .	3.2	32
137	A first search for coincident gravitational waves and high energy neutrinos using LIGO, Virgo and ANTARES data from 2007. Journal of Cosmology and Astroparticle Physics, 2013, 2013, 008-008.	5.4	32
138	Hollow and Concave Nanoparticles via Preferential Oxidation of the Core in Colloidal Core/Shell Nanocrystals. Journal of the American Chemical Society, 2014, 136, 9061-9069.	13.7	32
139	Optical properties of Yeast Cytochrome c monolayer on gold: An in situ spectroscopic ellipsometry investigation. Journal of Colloid and Interface Science, 2011, 364, 125-132.	9.4	31
140	CeO ₂ Nanoparticles-Loaded pH-Responsive Microparticles with Antitumoral Properties as Therapeutic Modulators for Osteosarcoma. ACS Omega, 2018, 3, 8952-8962.	3.5	31
141	Atomic Ligand Passivation of Colloidal Nanocrystal Films via their Reaction with Propyltrichlorosilane. Chemistry of Materials, 2013, 25, 1423-1429.	6.7	30
142	Graphene-Based Hole-Selective Layers for High-Efficiency, Solution-Processed, Large-Area, Flexible, Hydrogen-Evolving Organic Photocathodes. Journal of Physical Chemistry C, 2017, 121, 21887-21903.	3.1	30
143	Coating Evaporated MAPI Thin Films with Organic Molecules: Improved Stability at High Temperature and Implementation in High-Efficiency Solar Cells. ACS Energy Letters, 2018, 3, 835-839.	17.4	30
144	Reshaping the phonon energy landscape of nanocrystals inside a terahertz plasmonic nanocavity. Nature Communications, 2018, 9, 763.	12.8	30

#	Article	IF	CITATIONS
145	Nitrogen-doped graphene based triboelectric nanogenerators. Nano Energy, 2021, 87, 106173.	16.0	30
146	Status and perspectives of the Virgo gravitational wave detector. Journal of Physics: Conference Series, 2010, 203, 012074.	0.4	29
147	Nonâ€Equilibrium Synthesis of Highly Active Nanostructured, Oxygenâ€Incorporated Amorphous Molybdenum Sulfide HER Electrocatalyst. Small, 2020, 16, e2004047.	10.0	29
148	Moisture resistance in perovskite solar cells attributed to a water-splitting layer. Communications Materials, 2021, 2, .	6.9	29
149	The Seismic Superattenuators of the Virgo Gravitational Waves Interferometer. Journal of Low Frequency Noise Vibration and Active Control, 2011, 30, 63-79.	2.9	28
150	Hydrothermal evolution of PF-co-doped TiO2 nanoparticles and their antibacterial activity against carbapenem-resistant Klebsiella pneumoniae. Applied Catalysis B: Environmental, 2018, 231, 115-122.	20.2	28
151	Ruthenium-Decorated Cobalt Selenide Nanocrystals for Hydrogen Evolution. ACS Applied Nano Materials, 2019, 2, 5695-5703.	5.0	28
152	Single-/Few-Layer Graphene as Long-Lasting Electrocatalyst for Hydrogen Evolution Reaction. ACS Applied Energy Materials, 2019, 2, 5373-5379.	5.1	28
153	Flexible Graphene/Carbon Nanotube Electrochemical Double‣ayer Capacitors with Ultrahigh Areal Performance. ChemPlusChem, 2019, 84, 882-892.	2.8	28
154	POSS vapor phase grafting: a novel method to modify polymer films. Journal of Materials Chemistry, 2011, 21, 18049.	6.7	27
155	Tic-Tac-Toe Binary Lattices from the Interfacial Self-Assembly of Branched and Spherical Nanocrystals. ACS Nano, 2016, 10, 4345-4353.	14.6	27
156	Ceria/Gold Nanoparticles <i>in Situ</i> Synthesized on Polymeric Membranes with Enhanced Photocatalytic and Radical Scavenging Activity. ACS Applied Nano Materials, 2018, 1, 5601-5611.	5.0	27
157	Metallic Nanoporous Aluminum–Magnesium Alloy for UV-Enhanced Spectroscopy. Journal of Physical Chemistry C, 2019, 123, 20287-20296.	3.1	27
158	Control of electronic band profiles through depletion layer engineering in core–shell nanocrystals. Nature Communications, 2022, 13, 537.	12.8	27
159	From trash to resource: recovered-Pd from spent three-way catalysts as a precursor of an effective photo-catalyst for H ₂ production. Green Chemistry, 2016, 18, 2745-2752.	9.0	26
160	ITO nanoparticles break optical transparency/high-areal capacitance trade-off for advanced aqueous supercapacitors. Journal of Materials Chemistry A, 2017, 5, 25177-25186.	10.3	26
161	Ni–Co–S–Se Alloy Nanocrystals: Influence of the Composition on Their in Situ Transformation and Electrocatalytic Activity for the Oxygen Evolution Reaction. ACS Applied Nano Materials, 2018, 1, 5753-5762.	5.0	26
162	Single walled carbon nanohorns composite for neural sensing and stimulation. Sensors and Actuators B: Chemical, 2018, 271, 280-288.	7.8	26

#	Article	IF	CITATIONS
163	Pyramid-Shaped Wurtzite CdSe Nanocrystals with Inverted Polarity. ACS Nano, 2015, 9, 8537-8546.	14.6	25
164	Biobased System Composed of Electrospun sc-PLA/POSS/Cyclodextrin Fibers To Remove Water Pollutants. ACS Sustainable Chemistry and Engineering, 2015, 3, 2917-2924.	6.7	25
165	Colloidal Synthesis of Bipolar Off-Stoichiometric Gallium Iron Oxide Spinel-Type Nanocrystals with Near-IR Plasmon Resonance. Journal of the American Chemical Society, 2017, 139, 1198-1206.	13.7	25
166	Spectroscopic ellipsometry of self assembled monolayers: interface effects. The case of phenyl selenide SAMs on gold. Physical Chemistry Chemical Physics, 2013, 15, 11559.	2.8	24
167	Highly Effective Antiadhesive Coatings from pHâ€Modified Waterâ€Dispersed Perfluorinated Acrylic Copolymers: The Case of Vulcanizing Rubber. Advanced Materials Interfaces, 2016, 3, 1600069.	3.7	24
168	Understanding lead iodide perovskite hysteresis and degradation causes by extensive electrical characterization. Solar Energy Materials and Solar Cells, 2019, 189, 43-52.	6.2	24
169	Adhesive bonding of a mixed short and continuous carbon-fiber-reinforced Nylon-6 composite made via fused filament fabrication. International Journal of Adhesion and Adhesives, 2021, 107, 102856.	2.9	24
170	Cu ₂ Se and Cu Nanocrystals as Local Sources of Copper in Thermally Activated <i>In Situ</i> Cation Exchange. ACS Nano, 2016, 10, 2406-2414.	14.6	23
171	Tin Diselenide Molecular Precursor for Solutionâ€Processable Thermoelectric Materials. Angewandte Chemie - International Edition, 2018, 57, 17063-17068.	13.8	23
172	A New Drug Delivery System Based on Tauroursodeoxycholic Acid and PEDOT. Chemistry - A European Journal, 2019, 25, 2322-2329.	3.3	23
173	Engineering the Optical Emission and Robustness of Metalâ€Halide Layered Perovskites through Ligand Accommodation. Advanced Materials, 2021, 33, e2008004.	21.0	23
174	Inverted perovskite solar cells with enhanced lifetime and thermal stability enabled by a metallic tantalum disulfide buffer layer. Nanoscale Advances, 2021, 3, 3124-3135.	4.6	23
175	Multilayer poly(3,4-ethylenedioxythiophene)-dexamethasone and poly(3,4-ethylenedioxythiophene)-polystyrene sulfonate-carbon nanotubes coatings on glassy carbon microelectrode arrays for controlled drug release. Biointerphases, 2017, 12, 031002.	1.6	23
176	Hierarchical oxygen reduction reaction electrocatalysts based on FeSn0.5 species embedded in carbon nitride-graphene based supports. Electrochimica Acta, 2018, 280, 149-162.	5.2	22
177	Low-pressure plasma treatment of CFRP substrates for epoxy-adhesive bonding: an investigation of the effect of various process gases. International Journal of Advanced Manufacturing Technology, 2019, 102, 3021-3035.	3.0	22
178	"lon sliding―on graphene: a novel concept to boost supercapacitor performance. Nanoscale Horizons, 2019, 4, 1077-1091.	8.0	22
179	Nanopatterning by protein unfolding. Soft Matter, 2008, 4, 965.	2.7	21
180	Optical properties of uniform, porous, amorphous Ta ₂ O ₅ coatings on silica: temperature effects. Journal Physics D: Applied Physics, 2013, 46, 455301.	2.8	21

#	Article	IF	CITATIONS
181	"Quantized―Doping of Individual Colloidal Nanocrystals Using Size-Focused Metal Quantum Clusters. ACS Nano, 2017, 11, 6233-6242.	14.6	21
182	A two-fold engineering approach based on Bi ₂ Te ₃ flakes towards efficient and stable inverted perovskite solar cells. Materials Advances, 2020, 1, 450-462.	5.4	21
183	ZnCl ₂ Mediated Synthesis of InAs Nanocrystals with Aminoarsine. Journal of the American Chemical Society, 2022, 144, 10515-10523.	13.7	21
184	Dumbbell-like Au _{0.5} Cu _{0.5} @Fe ₃ O ₄ Nanocrystals: Synthesis, Characterization, and Catalytic Activity in CO Oxidation. ACS Applied Materials & Interfaces, 2016, 8, 28624-28632.	8.0	20
185	An efficient pure polyimide ammonia sensor. Journal of Materials Chemistry C, 2016, 4, 7790-7797.	5.5	20
186	Novel hybrid systems based on poly(propylene-g-maleic anhydride) and Ti-POSS by direct reactive blending. Polymer Degradation and Stability, 2011, 96, 1793-1798.	5.8	19
187	Selfâ€Assembled Dense Colloidal Cu ₂ Te Nanodisk Networks in P3HT Thin Films with Enhanced Photocurrent. Advanced Functional Materials, 2016, 26, 4535-4542.	14.9	19
188	Preparation, Characterization, and Preliminary In Vitro Testing of Nanoceria-Loaded Liposomes. Nanomaterials, 2017, 7, 276.	4.1	19
189	Dually responsive gold–iron oxide heterodimers: merging stimuli-responsive surface properties with intrinsic inorganic material features. Nanoscale, 2018, 10, 3930-3944.	5.6	19
190	Biochemically Controlled Release of Dexamethasone Covalently Bound to PEDOT. Chemistry - A European Journal, 2018, 24, 10300-10305.	3.3	19
191	Stem cell and tissue regeneration analysis in low-dose irradiated planarians treated with cerium oxide nanoparticles. Materials Science and Engineering C, 2020, 115, 111113.	7.3	19
192	A Photoresponsive Hybrid Nanomaterial Based on Graphene and Polyhedral Oligomeric Silsesquioxanes. European Journal of Inorganic Chemistry, 2012, 2012, 5282-5287.	2.0	18
193	Metal Nanoclusters with Synergistically Engineered Optical and Buffering Activity of Intracellular Reactive Oxygen Species by Compositional and Supramolecular Design. Scientific Reports, 2017, 7, 5976.	3.3	18
194	In Situ Dynamic Nanostructuring of the Cu–Ti Catalyst-Support System Promotes Hydrogen Evolution under Alkaline Conditions. ACS Applied Materials & Interfaces, 2018, 10, 29583-29592.	8.0	18
195	Increasing responsivity and air stability of PbS colloidal quantum dot photoconductors with iodine surface ligands. Nanotechnology, 2019, 30, 405204.	2.6	18
196	Insight on the Failure Mechanism of Sn Electrodes for Sodium-Ion Batteries: Evidence of Pore Formation during Sodiation and Crack Formation during Desodiation. ACS Applied Energy Materials, 2019, 2, 860-866.	5.1	18
197	Microwaveâ€Induced Structural Engineering and Pt Trapping in <i>6R</i> â€TaS ₂ for the Hydrogen Evolution Reaction. Small, 2020, 16, e2003372.	10.0	18
198	Influence of copper telluride nanodomains on the transport properties of n-type bismuth telluride. Chemical Engineering Journal, 2021, 418, 129374.	12.7	18

#	Article	IF	CITATIONS
199	Mixed Dimethylammonium/Methylammonium Lead Halide Perovskite Crystals for Improved Structural Stability and Enhanced Photodetection. Advanced Materials, 2022, 34, e2106160.	21.0	18
200	Oxygen Sensitivity of Atomically Passivated CdS Nanocrystal Films. ACS Applied Materials & Interfaces, 2014, 6, 9517-9523.	8.0	17
201	Specific Neuron Placement on Gold and Silicon Nitride-Patterned Substrates through a Two-Step Functionalization Method. Langmuir, 2016, 32, 6319-6327.	3.5	17
202	Bottomâ€up Synthesis and Selfâ€Assembly of Copper Clusters into Permanent Excimer Supramolecular Nanostructures. Angewandte Chemie - International Edition, 2018, 57, 7051-7055.	13.8	17
203	Quantized Electronic Doping towards Atomically Controlled "Charge-Engineered―Semiconductor Nanocrystals. Nano Letters, 2019, 19, 1307-1317.	9.1	17
204	Highly efficient sky-blue light-emitting diodes based on Cu-treated halide perovskite nanocrystals. Journal of Materials Chemistry C, 2020, 8, 13445-13452.	5.5	17
205	Colloidal Bismuth Chalcohalide Nanocrystals. Angewandte Chemie - International Edition, 2022, 61, .	13.8	17
206	Highly-efficient photocatalytic generation of superoxide radicals by phase-pure rutile TiO2 nanoparticles for azo dye removal. Applied Surface Science, 2019, 493, 719-728.	6.1	16
207	Revealing Photoluminescence Modulation from Layered Halide Perovskite Microcrystals upon Cyclic Compression. Advanced Materials, 2019, 31, e1805608.	21.0	16
208	Engineering Multiphase Metal Halide Perovskites Thin Films for Stable and Efficient Solar Cells. Advanced Energy Materials, 2020, 10, 1903221.	19.5	16
209	Photo-electrical properties of 2D quantum confined metal–organic chalcogenide nanocrystal films. Nanoscale, 2021, 13, 233-241.	5.6	16
210	Sustainable lithium-ion batteries based on metal-free tannery waste biochar. Green Chemistry, 2022, 24, 4119-4129.	9.0	16
211	Mercury Segregation and Diselenide Self-Assembly on Gold. Journal of Physical Chemistry C, 2012, 116, 2431-2437.	3.1	15
212	On stereocomplexed polylactide materials as support for PAMAM dendrimers: synthesis and properties. RSC Advances, 2015, 5, 46774-46784.	3.6	15
213	Extensive Characterization of Oxide-Coated Colloidal Gold Nanoparticles Synthesized by Laser Ablation in Liquid. Materials, 2016, 9, 775.	2.9	15
214	Nanosized, Hollow, and Mn-Doped CeO ₂ /SiO ₂ Catalysts via Galvanic Replacement: Preparation, Characterization, and Application as Highly Active Catalysts. ACS Applied Nano Materials, 2018, 1, 1438-1443.	5.0	15
215	Surface and interface engineering of anatase TiO2 anode for sodium-ion batteries through Al2O3 surface modification and wise electrolyte selection. Journal of Power Sources, 2018, 384, 18-26.	7.8	15
216	Cu underpotential deposition on Au controlled by in situ Spectroscopic Ellipsometry. Physica Status Solidi C: Current Topics in Solid State Physics, 2008, 5, 1304-1307.	0.8	14

#	Article	IF	CITATIONS
217	Metal-support interaction in catalysis: The influence of the morphology of a nano-oxide domain on catalytic activity. Applied Catalysis B: Environmental, 2018, 237, 753-762.	20.2	14
218	Hierarchical TiN Nanostructured Thin Film Electrode for Highly Stable PEM Fuel Cells. ACS Applied Energy Materials, 2019, 2, 1911-1922.	5.1	14
219	Impact of local structure on halogen ion migration in layered methylammonium copper halide memory devices. Journal of Materials Chemistry A, 2020, 8, 17516-17526.	10.3	14
220	Photoinduced Temperature Gradients in Subâ€Wavelength Plasmonic Structures: The Thermoplasmonics of Nanocones. Advanced Optical Materials, 2020, 8, 2000568.	7.3	14
221	Effect of the Counteranion on the Formation Pathway of Cu ₂ ZnSnS ₄ (CZTS) Nanoparticles under Solvothermal Conditions. Inorganic Chemistry, 2020, 59, 1973-1984.	4.0	14
222	Hybrid Organic/Inorganic Photocathodes Based on WS ₂ Flakes as Hole Transporting Layer Material. Small Structures, 2021, 2, 2000098.	12.0	14
223	Performance of the Virgo interferometer longitudinal control system during the second science run. Astroparticle Physics, 2011, 34, 521-527.	4.3	13
224	Gravitational waves detector mirrors: Spectroscopic ellipsometry study of Ta2O5 films on SiO2 substrates. Thin Solid Films, 2011, 519, 2877-2880.	1.8	13
225	Water-Based PEDOT:Nafion Dispersion for Organic Bioelectronics. ACS Applied Materials & Interfaces, 2020, 12, 29807-29817.	8.0	13
226	A robust and highly active hydrogen evolution catalyst based on Ru nanocrystals supported on vertically oriented Cu nanoplates. Journal of Materials Chemistry A, 2020, 8, 10787-10795.	10.3	13
227	Interaction of Alkanethiols with Nanoporous Cluster-Assembled Au Films. Langmuir, 2011, 27, 8371-8376.	3.5	12
228	The NoEMi (Noise Frequency Event Miner) framework. Journal of Physics: Conference Series, 2012, 363, 012037.	0.4	12
229	Core/Shell CdSe/CdS Boneâ€6haped Nanocrystals with a Thick and Anisotropic Shell as Optical Emitters. Advanced Optical Materials, 2020, 8, 1901463.	7.3	12
230	Photoluminescence enhancement and high accuracy patterning of lead halide perovskite single crystals by MeV ion beam irradiation. Journal of Materials Chemistry C, 2020, 8, 9923-9930.	5.5	12
231	Antibacterial Activity of Nanocrystalline TiO ₂ (B) on Multiresistant <i>Klebsiella pneumoniae</i> Strains. Science of Advanced Materials, 2013, 5, 1184-1192.	0.7	12
232	Understanding the Synthetic Pathway to Large-Area, High-Quality [AgSePh] _{â^ž} Nanocrystal Films. Journal of Physical Chemistry C, 2020, 124, 22845-22852.	3.1	11
233	Water-dispersible few-layer graphene flakes for selective and rapid ion mercury (Hg ²⁺)-rejecting membranes. Materials Advances, 2020, 1, 387-402.	5.4	11
234	Towards enhanced sodium storage of anatase TiO ₂ <i>via</i> a dual-modification approach of Mo doping combined with AlF ₃ coating. Nanoscale, 2020, 12, 15896-15904.	5.6	11

#	Article	IF	CITATIONS
235	Synthesis of yolk–shell Co ₃ O ₄ /Co _{1â^'x} Ru _x O ₂ microspheres featuring an enhanced electrocatalytic oxygen evolution activity in acidic medium. Journal of Materials Chemistry A, 2021, 9, 10385-10392.	10.3	11
236	Cleaning the Virgo sampled data for the search of periodic sources of gravitational waves. Classical and Quantum Gravity, 2009, 26, 204002.	4.0	10
237	Performances of the Virgo interferometer longitudinal control system. Astroparticle Physics, 2010, 33, 75-80.	4.3	10
238	Hydrothermal synthesis, structure and photocatalytic activity of PF-co-doped TiO2. Materials Science in Semiconductor Processing, 2015, 30, 442-450.	4.0	10
239	Photocatalytic Inactivation of Plant Pathogenic Bacteria Using TiO2 Nanoparticles Prepared Hydrothermally. Nanomaterials, 2020, 10, 1730.	4.1	10
240	Coupling of keratin with titanium: A physico-chemical characterization of functionalized or coated surfaces. Surface and Coatings Technology, 2020, 397, 126057.	4.8	10
241	Metastable CdTe@HgTe Core@Shell Nanostructures Obtained by Partial Cation Exchange Evolve into Sintered CdTe Films Upon Annealing. Chemistry of Materials, 2020, 32, 2978-2985.	6.7	10
242	Work Function Tuning in Hydrothermally Synthesized Vanadium-Doped MoO3 and Co3O4 Mesostructures for Energy Conversion Devices. Applied Sciences (Switzerland), 2021, 11, 2016.	2.5	10
243	Tuning the CO oxidation catalytic activity of supported metal–metal oxide heterostructures by an aqueous phase post-treatment process. Journal of Materials Chemistry A, 2016, 4, 18075-18083.	10.3	9
244	Tin Diselenide Molecular Precursor for Solutionâ€Processable Thermoelectric Materials. Angewandte Chemie, 2018, 130, 17309-17314.	2.0	9
245	Virgo calibration and reconstruction of the gravitationnal wave strain during VSR1. Journal of Physics: Conference Series, 2010, 228, 012015.	0.4	8
246	Mechanical characterization of â€~uncoated' and â€~Ta 2 O 5 -single-layer-coated' SiO 2 substrates: resul from GeNS suspension, and the CoaCh project. Classical and Quantum Gravity, 2010, 27, 084031.	^{ts} 4.0	8
247	In-vacuum Faraday isolation remote tuning. Applied Optics, 2010, 49, 4780.	2.1	8
248	A state observer for the Virgo inverted pendulum. Review of Scientific Instruments, 2011, 82, 094502.	1.3	8
249	Aligning Amyloid-Like Fibrils on Nanopatterned Graphite. BioNanoScience, 2012, 2, 75-82.	3.5	8
250	Compression stiffness of porous nanostructures from self-assembly of branched nanocrystals. Nanoscale, 2013, 5, 681-686.	5.6	8
251	Silica-supported pyrolyzed lignin for solid-phase extraction of rare earth elements from fresh and sea waters followed by ICP-MS detection. Analytical and Bioanalytical Chemistry, 2018, 410, 7635-7643.	3.7	8
252	Two‧tep Thermal Annealing: An Effective Route for 15 % Efficient Quasiâ€2D Perovskite Solar Cells. ChemPlusChem, 2021, 86, 1044-1048.	2.8	8

#	Article	IF	CITATIONS
253	Cerium Oxide Nanoparticle Administration to Skeletal Muscle Cells under Different Gravity and Radiation Conditions. ACS Applied Materials & Interfaces, 2021, 13, 40200-40213.	8.0	8
254	Self–assembled monolayers of organosulphur molecules bearing calix[4]arene moieties. Bioelectrochemistry, 2004, 63, 3-7.	4.6	7
255	Self-assembled monolayers of a novel diacetylene on gold. Applied Surface Science, 2005, 246, 403-408.	6.1	7
256	Interaction of Liquids with Nanoporous Cluster Assembled Au Films. Journal of Physical Chemistry C, 2010, 114, 17591-17596.	3.1	7
257	Germanium Nanocrystals-MWCNTs Composites as Anode Materials for Lithium Ion Batteries. ECS Transactions, 2014, 62, 19-24.	0.5	7
258	Au _{1â^'x} Cu _x colloidal nanoparticles synthesized via a one-pot approach: understanding the temperature effect on the Au : Cu ratio. RSC Advances, 2016, 6, 22213-22221.	3.6	7
259	Facile purification protocol of CsPbBr3 nanocrystals for light-emitting diodes with improved performance. Optical Materials: X, 2022, 13, 100124.	0.8	7
260	Automatic Alignment system during the second science run of the Virgo interferometer. Astroparticle Physics, 2011, 34, 327-332.	4.3	6
261	Yeast Cytochrome c Monolayer on Flat and Nanostructured Gold Films Studied by UV–Vis Spectroscopic Ellipsometry. BioNanoScience, 2011, 1, 210-217.	3.5	6
262	(Co, Ni)Sn _{0.5} Nanoparticles Supported on Hierarchical Carbon Nitrideâ€Grapheneâ€Based Electrocatalysts for the Oxygen Reduction Reaction. ChemElectroChem, 2018, 5, 2029-2040.	3.4	6
263	Design of catalytically active porous gold structures from a bottom-up method: The role of metal traces in CO oxidation and oxidative coupling of methanol. Journal of Catalysis, 2019, 375, 279-286.	6.2	6
264	Characterization of the Virgo seismic environment. Classical and Quantum Gravity, 2012, 29, 025005.	4.0	5
265	Linear Discriminant Functions to Improve the Glaucoma Probability Score Analysis to Detect Glaucomatous Optic Nerve Heads. Journal of Glaucoma, 2013, 22, 73-79.	1.6	5
266	Long-term optical and morphological stability of CsPbBr3 nanocrystal-based films. Materials Research Bulletin, 2021, 134, 111107.	5.2	5
267	Phase evolution of Cu ₂ ZnSnS ₄ (CZTS) nanoparticles from <i>in situ</i> formed binary sulphides under solvothermal conditions. CrystEngComm, 2021, 23, 7944-7954.	2.6	5
268	Colloidal Bismuth Chalcohalide Nanocrystals. Angewandte Chemie, 2022, 134, .	2.0	5
269	Control of the laser frequency of the Virgo gravitational wave interferometer with an in-loop relative frequency stability of 1.0 ${\rm \AA}-$ 10â $^{\circ}21$ on a 100 ms time scale. , 2009, , .		4
270	Multitechnique investigation of Ta ₂ O ₅ films on SiO ₂ substrates: Comparison of optical, chemical and morphological properties. Journal of Physics: Conference Series, 2010, 228, 012020.	0.4	4

#	Article	IF	CITATIONS
271	THE VIRGO INTERFEROMETER FOR GRAVITATIONAL WAVE DETECTION. International Journal of Modern Physics D, 2011, 20, 2075-2079.	2.1	4
272	Bottomâ€up Synthesis and Selfâ€Assembly of Copper Clusters into Permanent Excimer Supramolecular Nanostructures. Angewandte Chemie, 2018, 130, 7169-7173.	2.0	4
273	Macroscopic Versus Microscopic Schottky Barrier Determination at (Au/Pt)/Ge(100): Interfacial Local Modulation. ACS Applied Materials & Interfaces, 2020, 12, 28894-28902.	8.0	4
274	Direct production of hydrogen peroxide over bimetallic CoPd catalysts: Investigation of the effect of Co addition and calcination temperature. Green Energy and Environment, 2023, 8, 246-257.	8.7	4
275	Antimicrobial Surfaces for Applications on Confined Inhabited Space Stations. Advanced Materials Interfaces, 2021, 8, 2100118.	3.7	4
276	Artificially altered gravity elicits cell homeostasis imbalance in planarian worms, and cerium oxide nanoparticles counteract this effect. Journal of Biomedical Materials Research - Part A, 2021, 109, 2322-2333.	4.0	4
277	Publisher's Note: All-sky search for gravitational-wave bursts in the first joint LIGO-GEO-Virgo run [Phys. Rev. D 81 , 102001 (2010)]. Physical Review D, 2012, 85, .	4.7	3
278	Comparative characterization of the surface state of Ti-6Al-4V substrates in different pre-bonding conditions. Journal of Advanced Joining Processes, 2021, 3, 100058.	2.7	3
279	Noise monitor tools and their application to Virgo data. Journal of Physics: Conference Series, 2012, 363, 012024.	0.4	2
280	Publisher's Note: Search for gravitational waves from compact binary coalescence in LIGO and Virgo data from S5 and VSR1 [Phys. Rev. D82, 102001 (2010)]. Physical Review D, 2012, 85, .	4.7	2
281	Porous Silicon as Nanostructured Anode Material for Lithium Ion Batteries. ECS Transactions, 2014, 62, 25-34.	0.5	2
282	Progress and challenges in advanced ground-based gravitational-wave detectors. General Relativity and Gravitation, 2014, 46, 1.	2.0	2
283	Solar Cells: Few-Layer MoS2Flakes as Active Buffer Layer for Stable Perovskite Solar Cells (Adv. Energy) Tj ETQq1	1 0,78431 19.5	14 ggBT /Ove
284	PbS Quantum Dots Decorating TiO2 Nanocrystals: Synthesis, Topology, and Optical Properties of the Colloidal Hybrid Architecture. Molecules, 2020, 25, 2939.	3.8	2
285	Graphite Nanopatterning Through Interaction with Bio-organic Molecules. Carbon Nanostructures, 2012, , 221-228.	0.1	2
286	A THERMAL COMPENSATION SYSTEM FOR THE GRAVITATIONAL WAVE DETECTOR VIRGO. , 2012, , .		2
287	Status of the commissioning of the Virgo interferometer. , 2012, , .		1
288	Conical nanoantenna arrays for terahertz light. , 2016, , .		1

Conical nanoantenna arrays for terahertz light. , 2016, , . 288

#	Article	IF	CITATIONS
289	PLANS FOR THE UPGRADE OF THE GRAVITATIONAL WAVE DETECTOR VIRGO: ADVANCED VIRGO. , 2012, , .		1
290	One-step functionalization of mildly and strongly reduced graphene oxide with maleimide: an experimental and theoretical investigation of the Diels–Alder [4+2] cycloaddition reaction. Physical Chemistry Chemical Physics, 2022, 24, 2491-2503.	2.8	1
291	Tools for noise characterization in Virgo. Journal of Physics: Conference Series, 2010, 243, 012004.	0.4	0
292	PROGRESSES IN THE REALIZATION OF A MONOLITHIC SUSPENSION SYSTEM IN VIRGO. , 2012, , .		0
293	Publisher's Note: Search for gravitational waves from binary black hole inspiral, merger, and ringdown [Phys. Rev. D83, 122005 (2011)]. Physical Review D, 2012, 85, .	4.7	0
294	Nanoantenna Enhanced Terahertz Spectroscopy of a Monolayer of Cadmium Selenide Quantum Dots. , 2014, , .		0
295	Resonant metallic nanostructures for enhanced terahertz spectroscopy. , 2015, , .		0
296	Modifying the Optical Phonon Response of Nanocrystals inside Terahertz Plasmonic Nanocavities. , 2019, , .		0
297	NOISE ANALYSIS IN VIRGO: ON-LINE AND OFFLINE TOOLS FOR NOISE CHARACTERIZATION. , 2012, , .		0